Fish and Shellfish Immunology Reports 3 (2022) 100064

Contents lists available at ScienceDirect

Fish and Shellfish Immunology Reports

journal homepage: www.sciencedirect.com/journal/fish-and-shellfish-immunology-reports

The expression profile of a multi-stress inducible transient receptor potential vanilloid 4 (TRPV4) in Pacific oyster *Crassostrea gigas*

Zhaoyu He [a,b,c], Chuanyan Yang [a,b,c,*], Dongli Jiang [a,b,c], Xiangbo Wang [a,b,c], Zhen Xing [a,b,c], Simiao Yu [a,b,c], Qian Yang [a,b,c], Lingling Wang [a,b,c,**]

[a] Liaoning Key Laboratory of Marine Animal Immunology & Disease Control, Dalian Ocean University, 52 Heishijiao Street, Dalian 116023, China
[b] Liaoning Key Laboratory of Marine Animal Immunology, Dalian Ocean University, Dalian 116023, China
[c] Dalian Key Laboratory of Aquatic Animal Disease Prevention and Control, Dalian Ocean

ARTICLE INFO

Keywords:
Crassostrea gigas
Transient receptor potential vanilloid 4
Expression profile
High temperature stress
Vibrio splendidus stimulation

ABSTRACT

Transient receptor potential vanilloid 4 (TRPV4) is one of the major non-selective cation channel proteins, which plays a crucial role in sensing biotic and abiotic stresses, such as pathogen infection, temperature, mechanical pressure and osmotic pressure changes by regulating Ca^{2+} homeostasis. In the present study, a TRPV4 homologue was identified in Pacific oyster *Crassostrea gigas*, designated as *Cg*TRPV4. The open reading frame (ORF) of *Cg*TRPV4 was of 2298 bp encoding a putative polypeptide of 765 amino acid residues with three typical ankyrin domains and six conserved transmembrane domains of TRPV4 subfamily proteins, as well as multiple N-glycosylation sites, cAMP- and cGMP-dependent protein kinase phosphorylation sites, protein kinase C phosphorylation sites, casein kinase II phosphorylation sites, and prokaryotic membrane lipoprotein lipid attachment site. The deduced amino acid sequence of *Cg*TRPV4 shared 20.5%-26.2% similarity with TRPV4s from other species. During the early ontogenesis stages of oyster, the mRNA transcripts of *Cg*TRPV4 were detectable in all the stages with the highest expression level in fertilized eggs and the lowest in D-hinged larvae. In adult oyster, the *Cg*TRPV4 mRNA could be detected in all the examined tissues, including gill, hepatopancreas, adductor muscle, labial palp, mantle and haemocyte, with the highest expression level in gill (45.08-fold of that in hepatopancreas, $p < 0.05$). In immunocytochemical assay, the *Cg*TRPV4 positive signals were distributed in both endoplasmic reticulum and cytoplasmic membrane of oyster haemocytes. The mRNA expression of *Cg*TRPV4 in gill was significantly up-regulated after high temperature stress at 30°C ($p < 0.05$) and after *Vibrio splendidus* stimulation ($p < 0.05$). These results indicated that *Cg*TRPV4 was a classical member of TRPV4 family in oyster, which was induced by either biotic or abiotic stimulations and involved in mediating the stress response of oysters.

1. Introduction

Transient receptor potential (TRP) channel is a class of non-selective cation channel proteins containing six transmembrane domains, and forms ion channels in the form of homologous or heterotetramers to regulate intracellular calcium homeostasis [1]. According to different structural characteristics, TRP superfamily can be divided into seven subfamilies, including TRPC (C stands for canonical or classical), TRPV (V stands for the vanilloid receptor), TRPM (M stands for melastatin), TRPA (A stands for the protein denoted ankyrin-like with transmembrane domains), TRPP (P stands for polycystin), TRPN (N stands for the no mechanoreceptor potential C) and TRPML (ML stands for mucolipin) subfamily [1]. The TRPV subfamily is named for its ability to be activated by chemicals containing vanilloid groups. By far, a total of six subfamily members have been identified (named TRPV1–6), among which TRPV4 is mostly studied.

Studies in model animals including mouse, human, nematode and fruit fly have shown that TRPV4 plays vital roles in sensing biotic stresses (such as pathogenic bacteria) and abiotic stresses (such as temperature, mechanical pressure, chemical pressure, and osmotic pressure) [2]. The classical TRPV4 is consisted of a conserved six transmembrane helical domain at the C-terminal and three to five

* Corresponding authors at: Liaoning Key Laboratory of Marine Animal Immunology & Disease Control, Dalian Ocean University, 52 Heishijiao Street, Dalian 116023, China.
** Corresponding author.
E-mail addresses: yangchuanyan@dlou.edu.cn (C. Yang), linglingwang@dlou.edu.cn (L. Wang).

https://doi.org/10.1016/j.fsirep.2022.100064
Received 5 August 2022; Received in revised form 11 August 2022; Accepted 12 August 2022
Available online 15 August 2022

ankyrin repeats (ANK) domains at the N-terminal [3], in which the latter ANK domain plays an important role in the assembly and transportation of TRPV4 [4], and determines the sensitivity of TRPV4 channel [5,6]. In mammalian, TRPV4 is broadly expressed in various tissues such as heart, arteries, lung, skin, bone, brain, urinary bladder, kidney, intestine, liver and pancreas, as well as in a wide range of cells such as neuron cells, epidermal cells, macrophages, and muscle cells [7–12]. The TRPV4 in different types of cells may play different functions in a variety of physiological and biochemical processes, such as signal transduction between neuron cells, endoplasmic reticulum (ER) stress, lipid peroxidation, inflammatory response, phagocytosis, and so on [13–16]. Compared to the vast knowledge on TRPV4 channel regulation, little is known about the induction mechanism of TRPV4 transcription [17].

Compared with the relatively in-depth research in model animals, the research on TRPVs in aquatic animals is very limited, mainly focusing on the identification of fish and shellfish TRPV subfamily members and analysis of their expression levelunder osmotic pressure [18–23,26], mechanical pressure [19,24], and temperature stress [23, 25,26]. At present, TPRV4s have been identified in zebra fish *Danio rerio*, half-smooth tongue sole *Cynoglossus semilaevis*, chum salmon *Oncorhynchus keta*, tilapia *Oreochromis mossambicus*, sea bass *Dicentrarchus labrax*, and Pacific oyster *Crassostrea gigas* [18–26]. Similar to their homologues in mammals, aquatic TRPV4s all harbor typical six transmembrane domains and three ANK domains [18–26]. The *Dr*TRPV4 is expressed in various sensory cells of *Danio rerio* such as retinal cells, ciliated sensory neurons, lateral line cells, and many tissues such as brain, kidney and heart, and its expression is affected by external osmotic pressure, drugs and other factors [19–22]. The *Ol*TRPV4 can be activated by agonist GSK1016790A, hypotonic solution, and temperature (cold and hot) stimulation [23]. *Dl*TRPV4 and *Cs*TRPV4 is involved in sensing osmotic pressure and mechanical stimulation, respectively [22,24]. The expression level of *Cg*TRPV4.7 mRNA in gill was higher than in other tissues, which can be induced by high temperature stress [25]. Interestingly, *Ok*TRPV4 generates two transcript variants through alternative splicing, TRPV4 x1 and TRPV x2, and their expression levels significantly increased with the increase of salinity and temperature and the decrease of temperature, respectively [26]. However, the functional characters and regulation mechanism of TRPV4s in aquatic animals especially in lower aquatic invertebrates under various stressors are still not clear.

The Pacific oysters *C. gigas*, a typical representative of intertidal organisms, have to cope with a series of biotic threats such as pathogens, and has been regarded as an attractive experimental model for studying the mechanism of environmental adaptation [27,28]. Timely sensing various stresses and triggering signaling pathways to induce the transcription of a variety of immune effectors may one of the important adaptation mechanisms for oyster *C. gigas*. Considering the important role of TRPV4s in sensing biotic and abiotic stresses and regulating the calcium homeostasis, a TRPV4 was identified from oyster *C. gigas* (*Cg*TRPV4) in the present study with the objectives to clarify its structural characteristics and investigate its expression profile under various stresses.

2. Materials and methods

2.1. Oysters and sample collection

All experiments were performed in accordance with the approval and guidelines of the Ethics Review Committee of Dalian Ocean University.

Two-year-old Pacific oysters *C. gigas* with an average shell length of 12–14 cm were collected from a commercial farm in Dalian, China. They were cultured in aerated seawater at 16°C for seven days and fed with diatom once a day before following experiments. Tissues including gill, muscle, labial palp, hepatopancreas and mantle were collected from six oysters as parallel samples, and haemolymph from these oysters was extracted and centrifuged at 800 × *g*, 4°C for 10 min to harvest the haemocyte. After addition of 1 mL Trizol reagent (Invitrogen), all the samples were stored at -80°C for further RNA extraction.

2.2. RNA extraction, gene cloning and sequence analysis of CgTRPV4

Total RNA isolation, cDNA synthesis and gene cloning were performed according to the previous reports [29]. The primers of *Cg*TRPV4-F and *Cg*TRPV4-R (Table 1) were designed according to the sequence information of *Cg*TRPV4 (GenBank accession No. XM_034442984.1). The PCR product was gel-purified, cloned into pMD19-T simple vector (Takara), and confirmed by DNA sequencing.

The conserved domains of*Cg*TRPV4 were predicted using the simple modular architecture research tool (SMART) (http://smart.embl-heidelberg.de/), and the conserved domain database (CDD) (https://www.ncbi.nlm.nih.gov/cdd). The amino acid sequence analyses were carried out using the BLAST algorithm (http://www.ncbi.nlm.nib.gov/BLAST). Multiple sequence alignments were conducted using the Cluster X 1.81 program. The molecular weight and hydrophobicity of *Cg*TRPV4 were predicted using the ProtParam Tool (https://web.expasy.org/protparam/). The secondary structure was predicted using the SOPMA (https://npsa-prabi.ibcp.fr/NPSA/npsa_sopma.html). The N-glycosylation site, cAMP- and cGMP-dependent protein kinase phosphorylation site, Protein kinase C phosphorylation site, Casein kinase II phosphorylation site and Prokaryotic membrane lipoprotein lipid attachment site were predicted using the SoftBerry-Psite (http://linux1.softberry.com/berry.phtml?topic=psite&group=programs&subgroup=proloc). The neighbor-joining (NJ) phylogenetic tree of *Cg*TRPV4 was constructed using MEGA 6.0 software. Bootstrap trials were replicated 1000 times to derive the confidence value for phylogeny analysis [24].

2.3. Detection of CgTPRV4 mRNA transcripts in different developmental stages of oyster larvae using quantitative real-time PCR (qRT-PCR)

All embryos and larvae were sampled from the Yipintang farm in Dalian, Liaoning Province, China in May, 2022 as previously described [30]. Briefly, the embryo or larvae at different stages were identified microscopically and collected as fertilized eggs, 4-cell embryos, 8-cell embryos, morula (6 h post-fertilization, hpf), blastula (11 hpf), gastrula (18 hpf), trochophore (22 hpf), D-hinged larvae (2 day post-fertilization, dpf). For each developmental stage, six aliquot samples were collected, re-suspended in 1 mL Trizol reagent (Invitrogen), and stored in liquid nitrogen immediately. RNA isolation and cDNA synthesis were carried out as described above. The cDNA mix was diluted to1:100 and stored at -80°C for subsequent SYBR Green qRT-PCR.

The mRNA transcripts of *Cg*TPRV4 in different tissues were analyzed by SYBR Green qRT-PCR. All reactions were performed as previously described [31]. The information of the gene specific primers for *Cg*TRPV4 (*Cg*TRPV4-RTFand *Cg*TRPV4-RTR) and *Cg*EF-α (*Cg*EF-α-RTF and *Cg*EF-α-RTR) used in the qRT-PCR was shown in Table 1. The expression of *Cg*TPRV4 was normalized to that of the elongation factor α

Table. 1
Sequences of the primers used in the test.

Primer name	Primer Sequence (5′-3′)
*Primers for gene Cg*TRPV4 (Accession number XM_034442984.1)	
*Cg*TRPV4-ANK-F	ATGGAATCTTATCCATATAACCAA
*Cg*TRPV4-ANK-R	ATTTGAAATGCTTCTTTACGAGTA
*Cg*TRPV4-ANK-EX-F	CGCCATATGATGGAGTTTTATCAGTATAA
*Cg*TRPV4-ANK-EX-R	CCCAAGCTTATTTGAAATGCTTCTGTATGA
*Cg*TRPV4-ANK-RT-F	CCATCTCAACCCAAAACCAGG
*Cg*TRPV4-ANK-RT-R	GCAGATAATCGGAGTGGTGTC
*Primers for gene Cg*EF-α (Accession number NM_001305313.2)	
Cg-EF-α-RT-F	AGTCACCAAGGCTGCACAGAAAG
Cg-EF-α-RT-R	TCCGACGTATTTCTTTGCGATGT

Table. 2
Sequences used for the *Cg*TRPV4 alignment and phylogenetic analysis.

Protein name	Organism	Accession number
TRPV4	*Homo sapiens*	XP_011536936.2
TRPV4	*Mus musculus*	XP_011246537.1
TRPV4	*Gallus gallus*	NP_990023.2
TRPV4	*Xenopus tropicalis*	XP_002932129.1
TRPV4	*Physeter catodon*	XP_028336047.1
TRPV4	*Danio rerio*	XP_005165208.1
TRPV4	*Larimichthys crocea*	XP_019130016.1
TRPV4	*Oncorhynchus mykiss*	XP_021476679.1
TRPV4	*Salmo salar*	XP_014016243.1
TRPV4	*Monopterus albus*	XP_020449937.1
TRPV4	*Trichinella spiralis*	KRZ95620.1
TRPV4	*Crassostrea gigas*	XP_034298875.1

(*Cg*EF-α) gene (GenBank accession No. NM_001305313.2) for each sample, and the relative expression levels of *Cg*TRPV4 were analyzed using the comparative Ct method ($2^{-\triangle\triangle Ct}$ method) [31,32].

2.4. Detection of CgTPRV4 mRNA transcripts in different tissues of adult oysters using qRT-PCR

The mRNA transcripts of *Cg*TPRV4 in different tissues were analyzed by SYBR Green qRT-PCR. The SYBR Green qRT-PCR was carried out, and the relative expression level of *Cg*TRPV4 was analyzed as previously described [31,32].

2.5. Recombinant expression and polyclonal antibody preparation of CgTPRV4

Recombinant protein of *Cg*TRPV4 fused with GST tag was expressed in *Escherichia coli* using the pCold™-GST DNA vector (Takara). The cDNA sequence encoding the ANK domains of *Cg*TRPV4 was amplified using gene specific primers r*Cg*TRPV4-ANK-F and r*Cg*TRPV4-ANK-R (Table 1) with restriction enzyme sites *Nde* I and *Hind* III. The PCR products were digested, gel-purified, and ligated into the expression vector pCold-GST (Takara). The recombinant plasmids pCold™-GST-*Cg*TRPV4-ANK were extracted and transformed into *E. coli* Transetta (DE3). The positive transformants were cultured in LB medium and induced using Isopropyl β-D-1-Thiogalactopyranoside (IPTG), and the cell lysates were separated using SDS-polyacrylamide gel electrophoresis (SDS-PAGE). The purification of the recombinant protein of *Cg*TRPV4 (designated r*Cg*TRPV4) and the purity and concentration analysis of r*Cg*TRPV4 were performed as previously described [30].

To prepare polyclonal antibody, the purified r*Cg*TRPV4-ANK was subcutaneously stimulated six-week-old female mice according to the previous description [30]. The anti-r*CgTRPV4* serum was stored at -80°C for subsequent experiments.

2.6. Western blot analysis

Proteins were extracted from haemocytes of oysters as previous described [33]. The specificity of polyclonal antibody against endogenous *Cg*TRPV4 in haemocytes was examined using Western blot analysisas previously described [30]. The proteins extracted from haemocytes were separated using 15% SDS-PAGE. The antibodies against r*Cg*TRPV4 (1:1000 dilution) and the HRP-conjugated goat anti-mouse (1:2000 dilution, Sangon Biotech) were used as primary and secondary antibodies, respectively. The western lighting ECL substrate system (Thermo Scientific) was used to detect the immune-blotted protein bands of *Cg*TRPV4. The results were visualized using a chemiluminescent imaging system (Amersham Imager 600).

2.7. Immunofluorescence assay

Immunofluorescence assay was carried out to investigate the subcellular localization of *Cg*TRPV4 in haemocytes as previously described with some modification [34]. The haemocytes were collected from five oysters, re-suspended in L15 cell culture media, deposited on dishes precoated with poly-Lysine (a drop on each) in the wet chamber, and fixed with 4% paraformaldehyde. After blocked with 3% bovine serum albumin (BSA) at room temperature for 30 min, the samples were incubated with anti-r*Cg*TRPV4 (diluted 1:1000 (v/v) in 3% BSA) antibody at 37°C for 1 h. Alexa Fluor 488-conjugated goat anti-mouse IgG (Sangon, diluted 1:1500 in 3% BSA) was used separately to incubate with the samples at 37°C for 1 h. ER-Tracker Red (Beyotime, diluted 1:1500 in 3% BSA) and Dil (Beyotime, diluted 1:1000 in 3% BSA) were used to incubate with the samples to stain ER or the membrane. After incubated with 4, 6-diamidino-2-phenylindole hydrochloride (DAPI, diluted at 1:500 with 3% BSA) for 10 min to stain the nuclei, fluorescent images of the oyster haemocytes were obtained using a Laser Scan Confocal Microscope (ZEISS).

2.8. Analysis of CgTPRV4 mRNA expression under different temperature using qRT-PCR

The different temperature treatment was performed by transferring 60 oysters from aerated seawater at 16°C to aerated seawater at 22°C, 26°C, 30°C and 34°C. Nine oysters were sampled from each group at 12 h post-treatment, and the gill collected from three individuals were pooled together as one sample, and there were three samples for each time point. Nine untreated oysters were used as blank samples. The SYBR Green qRT-PCR was carried out, and the relative expression level of *Cg*TRPV4 was analyzed as previously described [30,31].

2.9. Analysis of CgTPRV4 mRNA expression after Vibrio splendidus stimulation using qRT-PCR

The *V. splendidus* stimulation experiment was performed as previously described [35]. Briefly, the oysters were sawed a narrowed notch in the oyster shell adjacent to the adductor muscle, and then were acclimated for one week. Seventy oysters were equally separated into two groups. The oysters in two groups received a 100 μL injection of sterile seawater and *V. splendidus* (1×10^9 CFU mL^{-1}) into the adductor muscle, respectively. Afterwards, nine oysters were sampled from each group at 0, 6 and 12 h post-injection, and the gill collected from three individuals were pooled together as one sample, and there were three samples for each time point. The SYBR Green qRT-PCR was carried out, and the relative expression level of *Cg*TRPV4 was analyzed as previously described [30,31].

2.10. Statistical analysis

All data were analyzed using ANOVA followed by a multiple comparison. The results were given as mean ± SD ($N \geq 4$), and statistically significant difference was designated at $p < 0.05$.

3. Results

3.1. Molecular characteristics and phylogenetic evolution of CgTRPV4

The open reading frame (ORF) of *Cg*TRPV4 was of 2298 bp, encoding a polypeptide of 765 amino acid residues with anisoelectric point (pI) of 8.52 and molecular weight (MW) of 89.3 kDa. There were three typical ANK domains and six transmembrane domains in *Cg*TRPV4 (Fig. 1). Furthermore, there were seven N-glycosylation sites ($NTNR_{138–141}$, $NKSG_{250–253}$, $NCTR_{327–330}$, $NETT_{388–391}$, $NRSV_{667–670}$, $NDTL_{710–713}$, $NKSS_{751–754}$), two cAMP- and cGMP-dependent protein kinase phosphorylation sites ($KRKT_{724–727}$, $KKSS_{731–734}$), ten protein kinase C phosphorylation sites ($SLR_{5–7}$, $TLR_{35–37}$, $TGK_{149–151}$, $STK_{239–241}$, $SAK_{260–262}$, $TRK_{329–331}$, $SVR_{669–671}$, $TDR_{672–674}$, $TKR_{723–725}$, $SSK_{733–735}$), nine casein kinase II phosphorylation sites ($TESE_{102–105}$,

A

```
1                                                    TTCATCATTGATTTTGGGTGATGCACTTGCATAGCCAGCAGTTTGTAGTAGGGGAAAATCGTCA
65   ATGCAAACTTGGAGCTTAAGAAAAGGCATGGAATCTTATCCATATAACCAAAAGAATGTGATCAAGACCTTGTGTTCTCACAATAAGGAT
1     M  Q  T  W  S  L  R  K  G  M  E  S  Y  P  Y  N  Q  K  N  V  I  K  T  L  C  S  H  N  K  D
155  GTTTTTCTTGATACCTTGAGGAGAATTATCAAAGAAAAAAGATTTGAAGCCGATTATGAGAGAGTAAATTTAGGAGTTAAAATAAAATGT
31    V  F  L  D  T  L  R  R  I  I  K  E  K  R  F  E  A  D  Y  E  R  V  N  L  G  V  K  I  K  C
245  AATGGAGAATCAATTTTGCATAGAGTATTAAAGTACAAAGATTCTGTTACACTCGAATTTGTTAAAAAGTTTGCGGGGGAAAAACCTGAA
61    N  G  E  S  I  L  H  R  V  L  K  Y  K  D  S  V  T  L  E  F  V  K  K  F  A  G  E  K  P  E
335  CTTTTAAAAGAGCTTAGAGATTCAAAAGAAGTTACGGAATCGGAAGTTAGCAACTTTCGGGGTCAATCTCCCCTGCACGTTGCAATAGTC
91    L  L  K  E  L  R  D  S  K  E  V  T  E  S  E  V  S  N  F  R  G  Q  S  P  L  H  V  A  I  V
425  AACGGATATGCTGACGCCGTTGAAGCAATTTTAAAAATTGCTGCTGAAAATAACATCACCCGAGAATTGCTTTGCATCCGTGCAACGGGT
121   N  G  Y  A  D  A  V  E  A  I  L  K  I  A  A  E  N  N  I  T  R  E  L  L  C  I  R  A  T  G
515  AAAAAATTCAAGAAGACGGTTTTAATGGGGCAGCTTCCATTGAGCGCCGCTGCTCTTGCTTGTAGGAACGAAGAATTTGAAATATTAGAT
151   K  K  F  K  K  T  V  L  M  G  Q  L  P  L  S  A  A  A  L  A  C  R  N  E  E  F  E  I  L  D
605  ATACTATTTAAAAATGATGCTATATATACTATTGCAAACCAAAACCAGGAAGGTGACACTGTATTTCACTCCTTGATCAAATATGCAGAT
181   I  L  F  K  N  D  A  I  Y  T  I  A  N  Q  N  Q  E  G  D  T  V  F  H  S  L  I  K  Y  A  D
695  ATTCATTCTGATCAAATGCAGCATATTGAGCCCACATTCACATTCATTTGGAATAAATTTTCCGAACAATGCAAAAAATCGAAGTCTACG
211   I  H  S  D  Q  M  Q  H  I  E  P  T  F  T  F  I  W  N  K  F  S  E  Q  C  K  K  S  K  S  T
785  AAAGTAACAGATATTCTTTTCTGGGAAAACAAATCAGGCATGACACCACTCCGATTATCTGCGAAACTTGGAGTCAGTGAGCTTTTTAAT
241   K  V  T  D  I  L  F  W  E  N  K  S  G  M  T  P  L  R  L  S  A  K  L  G  V  S  E  L  F  N
875  TATTTAATCAATATTGAAGGTGTCTACTGCTCTCCAAACATAAAAGATGGTCTCTTTGACATCAAGAAGTACGATGTAACTGAATTTGAT
271   Y  L  I  N  I  E  G  V  Y  C  S  P  N  I  K  D  G  L  F  D  I  K  K  Y  D  V  T  E  F  D
965  CGATTGATTAGCCATACAGAGAATTTGGAAGAATGTCAAAAACAAAAAATCTCAATTTTAGAGAGTGTTTTCGATTCAAATTGTACTCGT
301   R  L  I  S  H  T  E  N  L  E  E  C  Q  K  Q  K  I  S  I  L  E  S  V  F  D  S  N  C  T  R
1055 AAAGAAGCATTTCAAATTCTGAATCAAGAATTAGTAAAATTAATTCTGGATAAAAAATGGCGTACCTACCAGAAAGTCCTCATTCTTTGG
331   K  E  A  F  Q  I  L  N  Q  E  L  V  K  L  I  L  D  K  K  W  R  T  Y  Q  K  V  L  I  L  W
1145 ATGTTTCTACATATTATTTTCATGTGTTTTTTAACAACGACGACAATTGAAAAAACGAGGCATTATTTTCTTTCCCAGAACAATGAGACC
361   M  F  L  H  I  I  F  M  C  F  L  T  T  T  T  I  E  K  T  R  H  Y  F  L  S  Q  N  N  E  T
1235 ACGATTTCGTTTGATGTTGGAGAGTTTTCTACAGCAATAGTTTATATAGAATTGTTGATATTTTTGGTGGGCGGAATAACGTACCTTTTC
391   T  I  S  F  D  V  G  E  F  S  T  A  I  V  Y  I  E  L  L  I  F  L  V  G  G  I  T  Y  L  F
1325 TTCTTTTGTTTGTGTTTCAAAGAATTAGTCAGACGTTGTAGAGCGGAACAAGGAAGTCATTACAATTCTGGAATAATATTGCATAATTTTA
421   F  F  C  L  C  F  K  E  L  V  R  R  C  R  A  E  Q  G  S  H  Y  N  S  G  I  I  L  H  N  L
1415 GACTACATTGTGTGTTTATTGTTCACGTCTCTTGGTGCATTAGTAGAATCCGTCCTCTTTCCTCTCAAAATTCACTGGGACTATCATTTA
451   D  Y  I  V  C  L  L  F  T  S  L  G  A  L  V  E  S  V  L  F  P  L  K  I  H  W  D  Y  H  L
1505 GTATTTGCATTCATATCTGGCTGGTATTTTATGCTGTATTTCTCTCCTTTTCGAAAAGAAATCGTTTCTTTTACATACATGATAAAATCA
481   V  F  A  F  I  S  G  W  Y  F  M  L  Y  F  S  P  F  R  K  E  I  V  S  F  T  Y  M  I  K  S
1595 GGGTTTTTTGAAGATTTTGTTCCCTTTGCATCTGTTTATTGTTGTCTGTTGATTTCGTTCACAACAATTATGTTCATGCTTTTCCATGGC
511   G  F  F  E  D  F  V  P  F  A  S  V  Y  C  C  L  L  I  S  F  T  T  I  M  F  M  L  F  H  G
1685 GCGAATGATGTAGAAGACTTTGATAGCTTTGAAAGTTCCCTATTAGCGATGTTTAAATTAGGAGTAGGTTTGAATGACATAGGGATGCTG
541   A  N  D  V  E  D  F  D  S  F  E  S  S  L  L  A  M  F  K  L  G  V  G  L  N  D  I  G  M  L
1775 AATCAGGCTAGGATACCATGGCTTGCTCACACAATATTCGTAGTGTTTGTTGTTCTTTCATTCATTCATTTGTTCAACGCTTTGATTGCT
571   N  Q  A  R  I  P  W  L  A  H  T  I  F  V  V  F  V  V  L  S  F  I  H  L  F  N  A  L  I  A
1865 GTGATGTCACAGACCTTCTCTGGGGTTCATGATTATAGAAACTCTTACGCTCTATACAACAAATTAAGAATGATAGAATTGTTCGAAGAC
601   V  M  S  Q  T  F  S  G  V  H  D  Y  R  N  S  Y  A  L  Y  N  K  L  R  M  I  E  L  F  E  D
1955 ATAATTTTATTCAGGGTAAAATCAAAATACCCATTTAAACCTCTCTTTAACCGGGCAAAACATTGGAATAAAGATGATGATGACATTGAC
631   I  I  L  F  R  V  K  S  K  Y  P  F  K  P  L  F  N  R  A  K  H  W  N  K  D  D  D  D  I  D
2045 GATGAAATATCAATCGTTAACAGAAGCGTTAGAACGGATAGATTTAAAAATGGAAAACAAGAAAGACAGGTGCGCTTCTATTCTACAATG
661   D  E  I  S  I  V  N  R  S  V  R  T  D  R  F  K  N  G  K  Q  E  R  Q  V  R  F  Y  S  T  M
2135 GAGCTGGATGACCTGGAAGACAATAGAGATGACAAGGAAGAGAAGAAAAAGAAAATGAATGACACTTTGTCAAAGCACTTGCTTAAACAA
691   E  L  D  D  L  E  D  N  R  D  D  K  E  E  K  K  K  K  M  N  D  T  L  S  K  H  L  L  K  Q
2225 AGAGGAACTAAAAGAAAAACTCCAAATTTAAAGAAATCCAGCAAAACTAATCCCGAGAAAGATATAATATTCGTTAATATCCAAAAATGT
721   R  G  T  K  R  K  T  P  N  L  K  K  S  S  K  T  N  P  E  K  D  I  I  F  V  N  I  Q  K  C
2315 AACAAATCATCTCAATATCCAGAAGGCATTACACTTCCTAAATGGTAAATTAAATGCTGTCAAAGCGGCGTGGTCACGATTTTCTTAAAA
751   N  K  S  S  Q  Y  P  E  G  I  T  L  P  K  W  *
2405 TTTTACATTTCCATTGTTAATATTCTGATATGGTCGACTAAAATTTTTGTCAATTTTTCAGCTATATTATCTGATACAGAGCTCATATGT
2495 TTTTGTGAACATGATTACACAGTTTCTAGTGTTATCACTTCTTATCTTGATTTTTCAAATGCACTCTTTATCAAGCAATCTAGATGTAAA
2585 CAAACACATGGCTCGAACCATGTTTACATAGAATAAAATTATGGGCTCTGTTTACAACAAATGGTTAACGTTTGAATGGCCATTAGAAAT
2675 ACCGAAGTTAAGAATTTTGAACATTAAAAATAGAAAAGCAAAACTTTTTAAACAAAAAAAAACAAAAACCCATGTCCCTTGATGTCCAAC
2765 GTAAATACATCCTTGATTTGCAAAAAAAAA
```

B

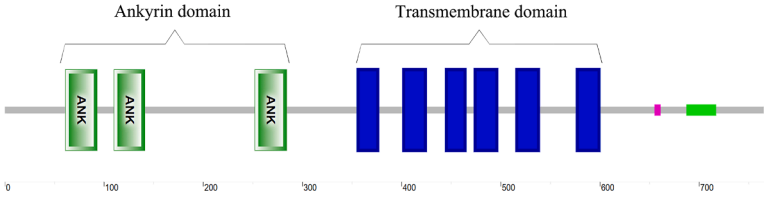

Fig. 1. Nucleotide, deduced amino acid sequence and protein domain of *Cg*TRPV4. (A) The nucleotide and deduced amino acid sequence of *Cg*TRPV4. The nucleotides and amino acid sequences are numbered along the left margin. The ANK domains and six transmembrane domains are marked with green and blue shadow. The Casein kinase II phosphorylation sites are marked by red letter. The N-glycosylation sites are marked by blue letter. The cAMP- and cGMP-dependent protein kinase phosphorylation sites are marked by green letter. The prokaryotic membrane lipoprotein lipid attachment site is marked by pink letter. (B) The domain structure of *Cg*TRPV4 analyzed by the SMART analysis and the CDD analysis.

TEFD$_{297–300}$, SHTE$_{304–307}$, SILE$_{318–321}$, SVFD$_{322–325}$, TRKE$_{329–332}$, TTIE$_{374–377}$, STME$_{688–691}$, TNPE$_{736–739}$), and one prokaryotic membrane lipoprotein lipid attachment site (QLPLSAAALAC$_{161–171}$), identified in *Cg*TRPV4 (Fig. 1).

Multiple sequence alignment revealed that *Cg*TRPV4 shared low similarity with TRPV4s from other organisms, including *Trichinella spiralis* (KRZ95620.1, 20.5%), *Homo sapiens* (XP_011536936.2, 21.3%), *Mus musculus* (XP_011246537.1, 22.8%), *Physeter catodon* (XP_028336047.1, 25.4%), *Monopterus albus* (XP_020449937.1, 25.7%), *Larimichthys crocea* (XP_019130016.1, 26.0%), *Xenopus tropicalis* (XP_002932129.1, 26.0%), *Danio rerio* (XP_005165208.1, 26.1%), *Salmo salar* (XP_014016243.1, 26.1%), *Gallus gallus* (NP_990023.2, 26.1%), and *Oncorhynchus mykiss* (XP_021476679.1, 26.2%). However, the ANK domains (27.1%-31.6%) and transmembrane domains (28.0%-36.8%) of *Cg*TRPV4 shared relatively higher similarity with their homologues from other organisms (Fig. 2).

The phylogenetic NJ trees were constructed to analyze the phylogenetic evolution of TRPV4s. Though *Cg*TRPV4 shared similar domain composition with other selected TRPV4s from vertebrates (*H. sapiens, M. musculus, P. catodon, G. gallus, L. crocea, M. albus, D. rerio, S.salar, O.*

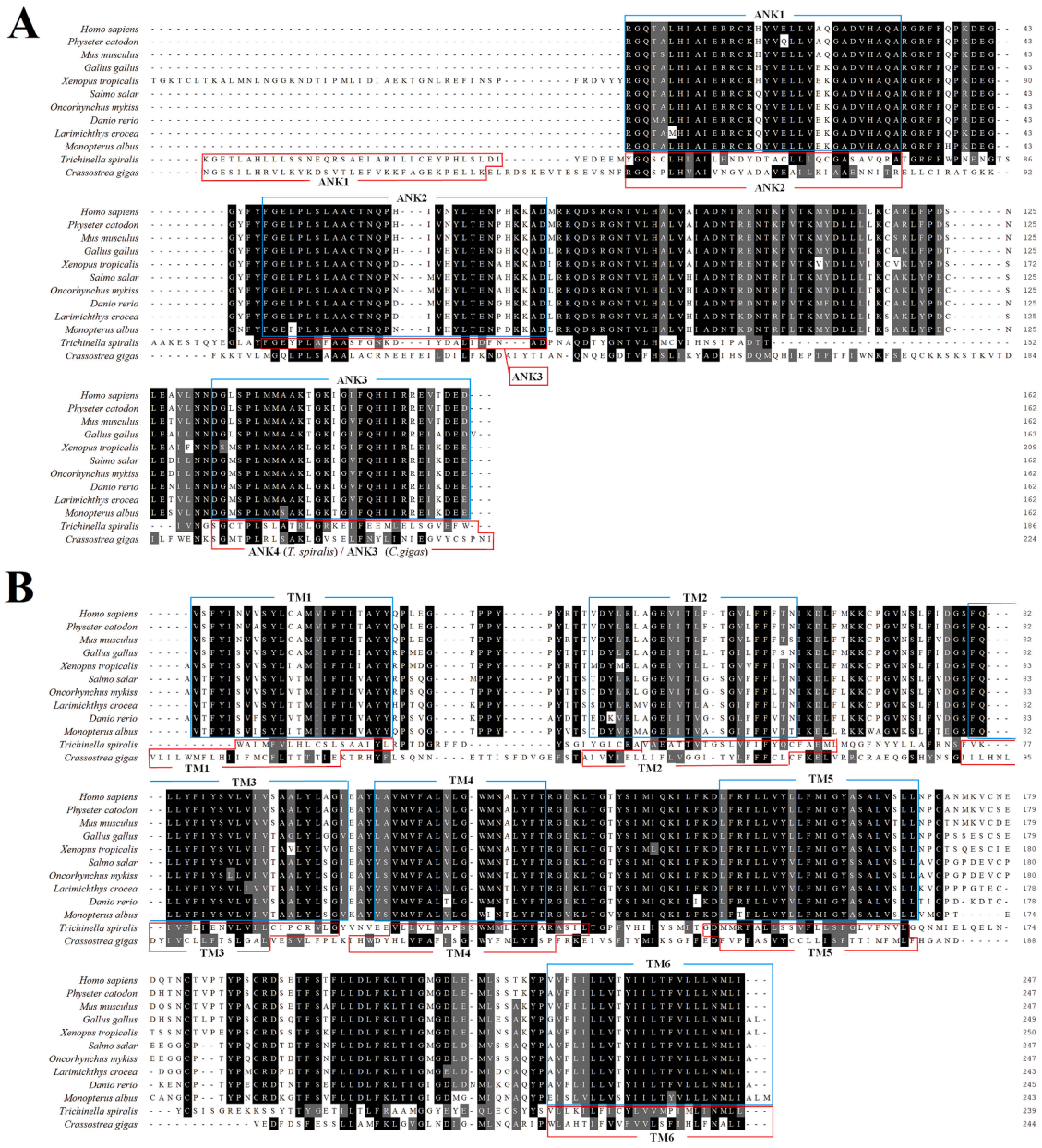

Fig. 2. Multiple sequence alignment of TRPV4s from invertebrate and vertebrate species. The identical amino acid residues of ANK domains (A) and transmembrane domains (B) of TRPV4s are shaded in black, and similar amino acids are shaded in dark gray. Sequence information of the TRPV4s is listed in Table 2.

mykiss and *X. tropicalis*) and invertebrate (*T. spiralis*), it showed relatively far evolutionary relationships with them (Fig. 3).

3.2. The mRNA expression of *Cg*TRPV4 in different developmental stages

In order to elucidate the possible role of *Cg*TRPV4 in the ontogenesis, its mRNA expression level in different development stages was monitored by qRT-PCR. The mRNA transcript of *Cg*TRPV4 was detected in the development stages from fertilized eggs to D-hinged larvae with the highest expression level in fertilized eggs (Fig. 4). The expression level of *Cg*TRPV4 decreased gradually in the following development stages and reached the lowest in D-hinged larvae (0.01-fold of that in fertilized eggs, $p < 0.05$) (Fig. 4).

3.3. The distribution of *Cg*TRPV4 mRNA in different tissues of adult oyster

The *Cg*TRPV4 transcripts were detected in all the examined tissues, including hepatopancreas, mantle, gill, muscle, labial palp and haemocyte. The highest mRNA expression level of *Cg*TRPV4 was detected in gill, which was 45.08-fold ($p < 0.05$) of that in the hepatopancreas (Fig. 5). The expression level of *Cg*TRPV4 mRNA in mantle (19.09-fold, $p < 0.05$) was also significantly higher than that in the hepatopancreas (Fig. 5).

3.4. The subcellular distribution of *Cg*TRPV4 in haemocytes

The cDNA sequence encoding the ANK domains of *Cg*TRPV4 was amplified and ligated into the pCold™-GST DNA vector (Fig. 6A). The recombinant plasmid (pCold-GST-*Cg*TRPV4-ANK) was transformed into *E. coli* Transetta (DE3). After IPTG induction for 4 h, the whole cell lysate

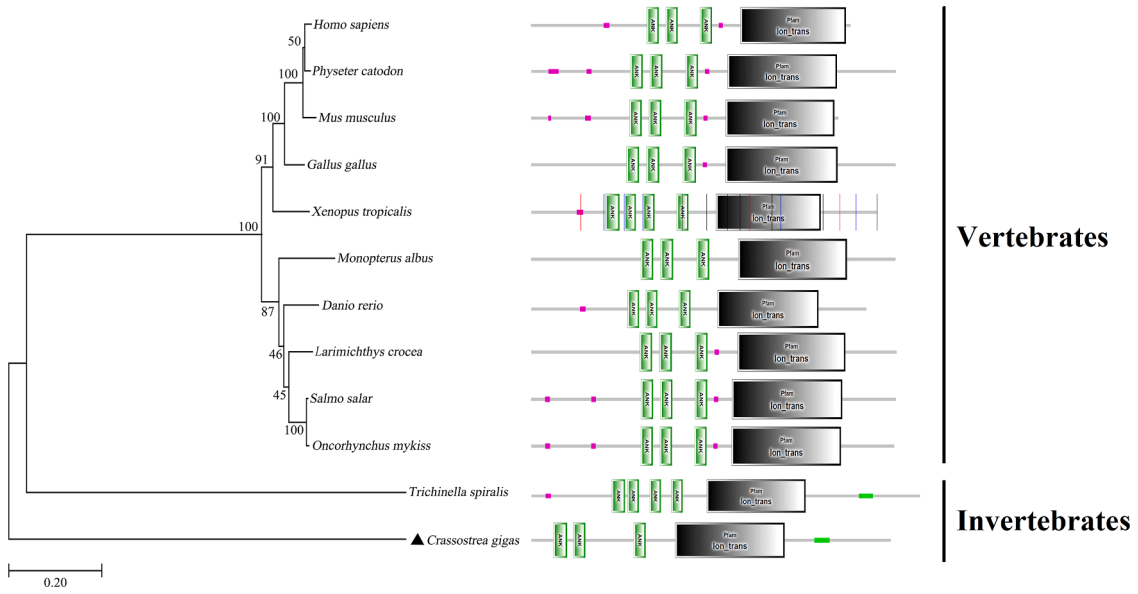

Fig. 3. The Neighbor-joining tree of*Cg*TRPV4. The *Cg*TRPV4 is marked with a triangle. Sequence information of the twelve TRPV4s is described in Table 2.

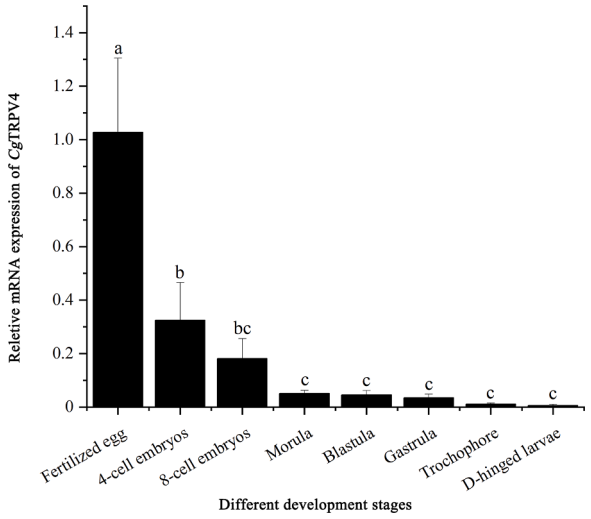

Fig. 4. The mRNA expression of *Cg*TRPV4 in different development stages. The relative mRNA expression level of *Cg*TRPV4 among different development stagesis normalized to that of *Cg*EF-α, and the significant difference is indicated by different letters (a, b and c). Each value is shown as mean ± S.D. (N ≥ 4).

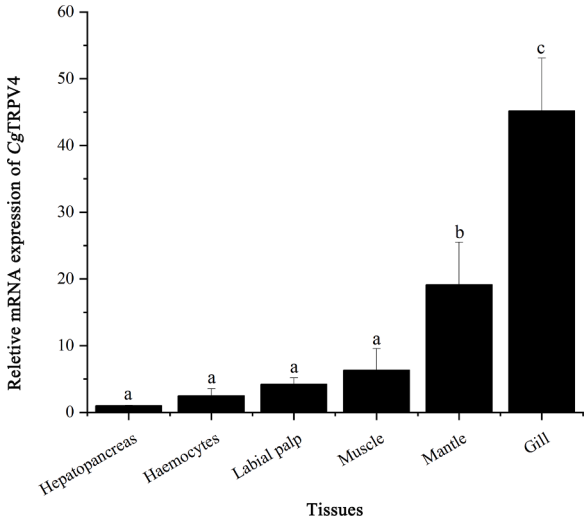

Fig. 5. The distribution of *Cg*TRPV4 mRNA in different tissues. The relative mRNA expression level of *Cg*TRPV4 among different tissues is normalized to that of *Cg*EF-α, and the significant difference is indicated by different letters (a, b and c). Each value is shown as mean ± S.D. (N ≥ 4).

was analyzed by SDS-PAGE, and a distinct band about 55.2 kDa was revealed, which was consistent with the predicted molecular weight of fusion r*Cg*TRPV4 with GST-tag (Fig. 6B, lane2). The r*Cg*TRPV4 was further purified for preparing the polyclonal antibody (Fig. 6B, lane3). The antibody specificity of the anti-r*Cg*TRPV4 was examined using endogenous protein of oyster haemocytes by Western blot analysis. A distinct immune-precipitated band with a molecular weight of approximately 89.30 kDa was revealed with a similar molecular weight predicted by the target sequence (Fig. 6C, lane1).

The subcellular distribution of *Cg*TRPV4 in oyster haemocytes was detected using immunofluorescence assay. The morphology of the haemocytes was observed in a bright field, and the nucleus stained by DAPI was shown in blue fluorescence. The positive signals of *Cg*TRPV4 labeled by FITC were indicated in green fluorescence, and both ER and cytoplasmic membrane labeled by ER-Tracker Red and Dil were indicated with red fluorescence. The co-localization of signals for *Cg*TRPV4 (green) and ER (red) was observed (Fig. 7). The co-localization of positive green signals for *Cg*TRPV4 and red signals for cytoplasmic membrane was also observable (Fig. 7), indicating that *Cg*TRPV4 were located in ER and cytoplasmic membrane of oyster haemocytes.

3.5. *Temporal expression of CgTRPV4 mRNA in gill under different temperature*

The expression profiles of *Cg*TRPV4 in gill at 12 h after different temperature treatment (22°C, 26°C, 30°C and 34°C) were investigated using qRT-PCR. The mRNA transcripts of *Cg*TRPV4 in gill were significantly up-regulated after high temperature stress at 30°C, which was 1.85-fold of that in the Blank group ($p < 0.05$). However, there was no significant difference between the blank group and the three experimental groups (22°C, 26°C and 34°C) (Fig. 8).

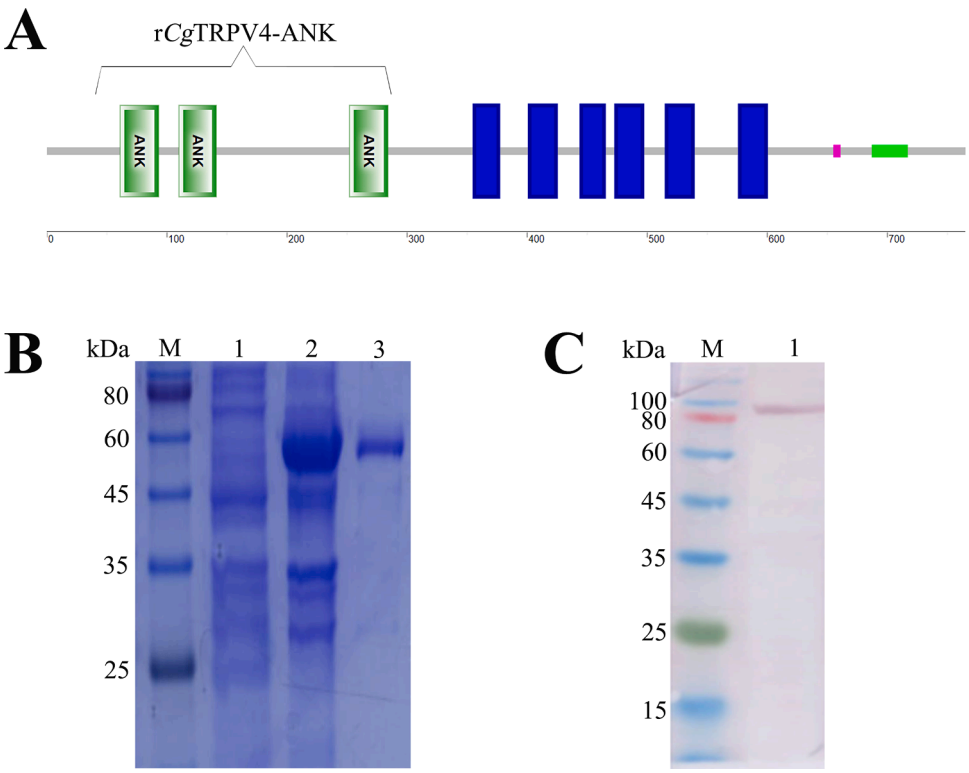

Fig. 6. SDS-PAGE and western blotting analysis of r*Cg*TRPV4. (A) The domain structure of *Cg*TRPV4 analyzed by the SMART analysis. (B) Lane M, protein molecular standard. Lane 1, negative control for r*Cg*TRPV4 (without induction). Lane 2, induced r*Cg*TRPV4. Lane 3, purified r*Cg*TRPV4. (C) Lane M, protein molecular standard. Lane 1, western blot analysis of the polyclonal antibody against endogenous of *Cg*TRPV4 in gill.

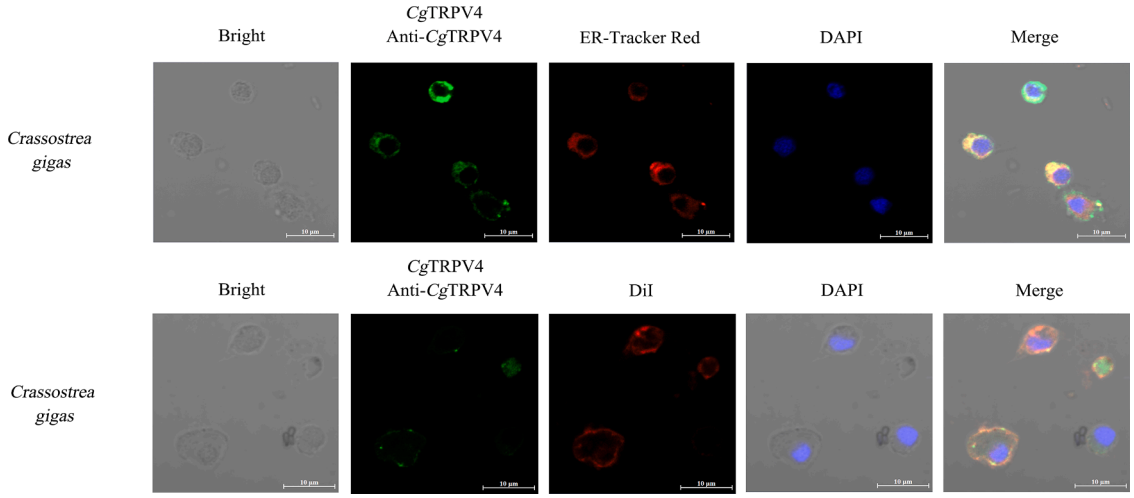

Fig. 7. Subcellular localization of *Cg*TRPV4 in haemocytes of *C. gigas*. The nuclei of haemocytes stained by DAPI were shown in blue fluorescence. The positive signals of *Cg*TRPV4 labeled by FITC were indicated in green fluorescence. Both ER and cytoplasmic membranes labeled by ER-Tracker Red and DiI were indicated in red fluorescence. Bar = 10 μm.

3.6. Temporal expression of CgTRPV4 mRNA in gill after V. splendidus stimulation

The expression profiles of *Cg*TRPV4 ingill after *V. splendidus* stimulation were investigated using qRT-PCR. Compared to the control group, the mRNA transcripts of *Cg*TRPV4 were significantly up-regulated at 6 h after *V. splendidus* stimulation (3.07-fold of that in the control group, $p < 0.05$). There wasno significant difference between the control group and the *V. splendidus* stimulation group at 0 h and 12 h post-stimulation (Fig. 9).

4. Discussion

TRPV4 usually plays an important role in sensing biological and abiotic stresses, such as pathogen infection, temperature, mechanical and osmotic pressure changes by regulating Ca^{2+} homeostasis [1,2,17]. In the present study, one TRPV4 was identified from Pacific oyster, which was consisted of three typical ANK domains and six transmembrane domains. The similar domain composition and conserved six transmembrane helical domains identified at the C-terminal of *Cg*TRPV4 and mammalian TRPV4s indicated that they might perform similar

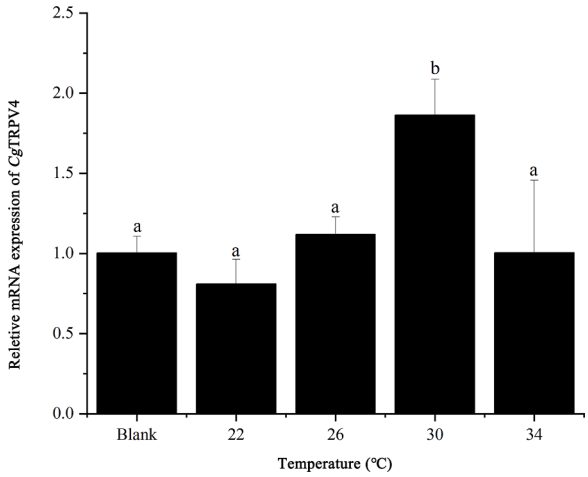

Fig. 8. The temporal expression of *Cg*TRPV4 mRNA in gill under different temperature. Relative expression levels of *Cg*TRPV4 mRNA in gill were normalized to that of *Cg*EF-α, and the significant difference is indicated by different letters (a and b). Each value is shown as mean ± S.D. (N ≥ 4).

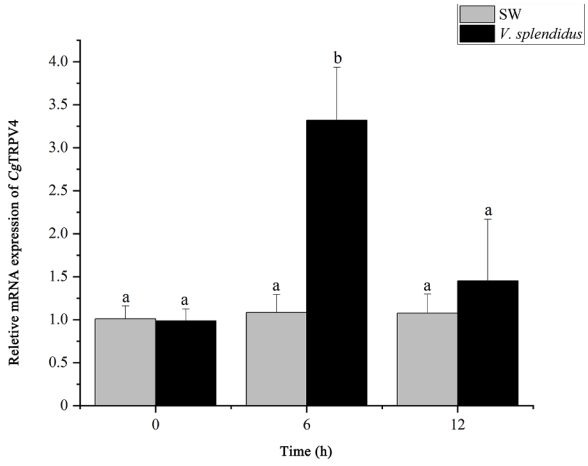

Fig. 9. The temporal expression of *Cg*TRPV4 mRNA in gill after *V. splendidus* stimulation. Relative expression levels of *Cg*TRPV4 mRNA in gill were normalized to that of *Cg*EF-α, and the significant difference is indicated by different letters (a, and b). Each value is shown as mean ± S.D. (N ≥ 4).

functions. Considering the important roles of ANK domain in the assemble and transportation of TRPV4 [3,4] as well as in determining the sensitivity of TRPV4 channel [5,6], the different number of ANK domains in *Cg*TRPV4 and mammalian TRPV4s indicated that there might be some functional differentiation between them. It was reported that N-glycosylation and phosphorylation regulated TRP destination to the specialized structures [36], and the phosphorylation of (cGMP)-dependent kinase protein kinase phosphorylation sites would inactivate TRP [37], while the phosphorylation of Casein kinase II site would modulate the function of TRP [38]. In addition to the typical domains and motifs, there were seven N-glycosylation sites, two cAMP- and cGMP-dependent protein kinase phosphorylation sites, ten protein kinase C phosphorylation sites, nine casein kinase II phosphorylation sites, and one prokaryotic membrane lipoprotein lipid attachment site identified in *Cg*TRPV4, suggesting that the activity of *Cg*TRPV4 is subjected to complex and precise regulation. In the phylogenetic NJ tree, the invertebrate TRPV4s (*Cg*TRPV4 and *Ts*TRPV4) showed relatively far evolutionary relationships with TRPV4s from other vertebrates, and this was consistent with the results of multiple sequence alignment, which revealed that *Cg*TRPV4 shared low similarity with TRPV4s from other organisms (20.5%-26.2%). The structural and evolutionary characteristics collectively suggested that *Cg*TRPV4 was a typical member of the TRPV4 family in invertebrates, which might be involved in regulating Ca^{2+} homeostasis similar to their homologues in other species, and meanwhile, there might be a certain degree of variation in *Cg*TRPV4.

TRPV4 is broadly expressed in various tissues and a wide range of cells in mammalian, and can be significantly regulated by either biotic or abiotic stimulations followed by the regulation of Ca^{2+} influx [7–16,18–26,39]. It is indicated that the mRNA expression profile of TRPV4 is associated with their physiological function. In order to further understand the potential function of *Cg*TRPV4, its expression profile in different development stages, different tissues and subcellular component of oyster haemocytes was investigated. The mRNA transcripts of *Cg*TRPV4 could be detected during the tested developmental stages with the highest level in fertilized eggs, and was significantly down-regulated from 4-cell embryos to D-hinged larvae. It was suspected that the higher level of *Cg*TRPV4 transcripts in fertilized eggs might be endowed by parents for the capability of sensing stress. It has been demonstrated that the immune tissues and organs of bivalves usually begin to form in gastrula and mature in D-hinged larvae and veliger larvae [40,41]. The level of *Cg*TRPV4 transcripts decreased along with the developmental stages, which may be explained by the observation that the sensory organs are not fully developed till D-hinged larvae. In the adult oysters, the *Cg*TRPV4 mRNA was constitutively expressed in all the examined tissues, and this wide distribution profile was consistent with that of mammalian TRPV4s [7–12]. Similar to *Cg*TRPV4.7 with incomplete domain composition [25], the highest mRNA expression level of *Cg*TRPV4 was also observed in gill, which function as the primarily sensitive tissue of molluscs responding to environmental stress [42,43]. These results indicated that TRPV4 might play a key role in resistance to environmental stress in oysters. The co-localization of *Cg*TRPV4 signals with ER and cytoplasmic membrane were observable, indicating that *Cg*TRPV4were located on both ER and cytoplasmic membrane of oyster haemocytes. This result was consistent with the subcellular localization of mouse TRPV4 [44], suggesting that *Cg*TRPV4 might function as a Ca^{2+} channel in both cytoplasmic membrane and ER membrane of oysters. These results collectively suggested that *Cg*TRPV4 might play a key role in resistance to environmental stress by regulating cytoplasmic Ca^{2+} homeostasis through channels on plasma membrane and ER membrane.

Accumulating evidences have shown that TRPV4 plays an important role in sensing both biotic and abiotic stresses [2]. In the present study, the expression profiles of *Cg*TRPV4 mRNA under different temperature or after *V. splendidus* stimulation was investigated to deduce its potential function. The mRNA transcripts of *Cg*TRPV4 in gill were significantly up-regulated after high temperature stress at 30°C, which favored the previous conclusion that TRPV4 is a temperature sensitive channel protein [2]. Similarly, the heat-induced mRNA expression of TRPV4s was also observed in other TRPV4s in aquatic animals, such as *Ol*TRPV4 [23], *Cg*TRPV4.7 [25] and *Ok*TRPV4 [26]. However, there was no significant change after high temperature stress at 34°C, probably due to the different temperature activation threshold of the thermoTRPV channels (TRPV1–4). The previous studies indicated that TRPV1–4 could be activated by temperatures ranging from innocuous warmth (< 37°C) to noxious heat (> 50°C) in heterologous systems [2,23,25,26,45]. It is suspected that four TRPV1s and eight TRPV4s identified in oyster genome may be responsible for sensing different temperature range [25]. In addition, the mRNA transcripts of *Cg*TRPV4 were significantly up-regulated at 6 h after *V. splendidus* stimulation. It was reported that the mammalian TRPV4 in different types of cells might play different functions in a variety of immune reaction, such as lipid peroxidation, inflammatory response, and phagocytosis [13–16]. The TRPV4 in airway epithelial cells and macrophages can be activated by LPS stimulation, which triggered downstream protective responses and anti-inflammatory pathways [13,14]. Moreover, TRPV4 could protect lung from injury upon intratracheal *Pseudomonas aeruginosa* in mice

through a novel mechanism of molecular switching of LPS signaling [46], and there was a significant increase in TRPV4 in the hippocampus of a depression mouse model induced by LPS [47]. These results indicated that *Cg*TRPV4 might share a similar role in sensing both biotic and abiotic stresses with their homologues in other species.

In conclusion, *Cg*TRPV4, a typical member of the TRPV4 family, was identified in Pacific oyster. The *Cg*TRPV4 transcripts were constitutively expressed in all the examined tissues with the highest expression level in gill, and *Cg*TRPV4 located in both ER and cytoplasmic membrane of oyster haemocytes. The expression level of *Cg*TRPV4 mRNA in gill was significantly up-regulated after high temperature stress at 30°C or *V. splendidus* stimulation. All above results indicated that *Cg*TRPV4 shared a similar role in sensing either biotic or abiotic stresses with their homologues in other species.

Declaration of Competing Interest

The authors have declared that no competing interests exist.

Acknowledgments

We are grateful to all the laboratory members for their technical advice and helpful discussions. This research was supported bythe National Key R&D Program (2018YFD0900601), a grant (No. 41961124009) from National Science Foundation of China, Liaoning Climbing Scholar, and the Distinguished Professor of Liaoning (XLYC1902012 to L. W.).

References

[1] T. Voets, K. Talavera, G. Owsianik, et al., Sensing with TRP channels, Nat. Chem. Biol. 1 (2) (2005) 85–92.
[2] J. Berrout, M. Jin, M. Mamenko, et al., Function of transient receptor potential cation channel subfamily V member 4 (TRPV4) as a mechanical transducer in flow-sensitive segments of renal collecting duct system, J. Biol. Chem. 287 (12) (2012) 8782–8791.
[3] B. Nilius, G. Owsianik, T. Voets, et al., Transient receptor potential cation channels in disease, Physiol. Rev. 87 (1) (2007) 165–217.
[4] A. Garcia-Elias, A. Berna-Erro, F. Rubio-Moscardo, et al., Interaction between the linker, pre-S1, and TRP domains determines folding, assembly, and trafficking of TRPV channels, Structure 23 (8) (2015) 1404–1413.
[5] C.B. Phelps, R.R. Wang, S.S. Choo, et al., Differential regulation of TRPV1, TRPV3, and TRPV4 sensitivity through a conserved binding site on the ankyrin repeat domain, J. Biol. Chem. 285 (1) (2010) 731–740.
[6] R. Potla, M. Hirano-Kobayashi, H. Wu, et al., Molecular mapping of transmembrane mechanotransduction through the β1 integrin–CD98hc–TRPV4 axis, J. Cell Sci. 133 (20) (2020), jcs248823.
[7] W. Everaerts, B. Nilius, G. Owsianik, The vanilloid transient receptor potential channel TRPV4: from structure to disease, Prog. Biophys. Mol. biol. 103 (1) (2010) 2–17.
[8] S. Rayees, J.C. Joshi, M. Tauseef, et al., PAR2-mediated cAMP generation suppresses TRPV4-dependent Ca^{2+} signaling in alveolar macrophages to resolve TLR4-induced inflammation, Cell Rep. 27 (3) (2019) 793–805, e4.
[9] N. Liu, J.Y. Liu, X.B. Wen, et al., TRPV4 contributes to ER stress: relation to apoptosis in the MPP^{+}-induced cell model of Parkinson's disease, Life Sci. 261 (2020), 118461.
[10] M. Nazıroğlu, A novel antagonist of TRPM2 and TRPV4 channels: carvacrol, Metab. Brain Dis. 37 (3) (2022) 711–728.
[11] A.H. Bubolz, S.A. Mendoza, X.D. Zheng, et al., Activation of endothelial TRPV4 channels mediates flow-induced dilation in human coronary arterioles: role of Ca^{2+} entry and mitochondrial ROS signaling, Am. J. Physiol. Heart Circ. Physiol. 302 (3) (2012) 634–642.
[12] J. Krüger, C. Kunert-Keil, F. Bisping, et al., Transient receptor potential cation channels in normal and dystrophic mdx muscle, Neuromuscul. Disord. 18 (6) (2008) 501–513.
[13] Y.A. Alpizar, B. Boonen, A. Sanchez, et al., TRPV4 activation triggers protective responses to bacterial lipopolysaccharides in airway epithelial cells, Nat. Commun. 8 (1) (2017) 1–13.
[14] R.G. Scheraga, S. Abraham, K.A. Niese, et al., TRPV4 mechanosensitive ion channel regulates lipopolysaccharide-stimulated macrophage phagocytosis, J. Immunol. 196 (1) (2016) 428–436.
[15] B. Dutta, R.K. Arya, R. Goswami, et al., Role of macrophage TRPV4 in inflammation, Lab. Investig. 100 (2) (2020) 178–185.
[16] M.R. Gao, J. Han, Y.F. Zhu, et al., Blocking endothelial TRPV4-Nox2 interaction helps reduce ROS production and inflammation, and improves vascular function in obese mice, J. Mol. Cell. Cardiol. 157 (2021) 66–76.
[17] B. Nilius, V. Flockerzi, Mammalian transient receptor potential (TRP) cation channels, Berlin, Germany (2014).
[18] A.P. Seale, S. Watanabe, J.P. Breves, et al., Differential regulation of TRPV4 mRNA levels by acclimation salinity and extracellular osmolality in euryhaline tilapia, Gen. Comp. Endocrinol. 178 (1) (2012) 123–130.
[19] V. Amato, E. Vina, M.G. Calavia, et al., TRPV4 in the sensory organs of adult zebrafish, Microsc. Res. Tech. 75 (1) (2012) 89–96.
[20] S. Watanabe, A.P. Seale, E.G. Grau, et al., Stretch-activated cation channel TRPV4 mediates hyposmotically induced prolactin release from prolactin cells of mozambique tilapia Oreochromis mossambicus, Am. J. Physiol. Regul. 302 (8) (2012) 1004–1011. Integrative Comparative Physiology.
[21] S. Mangos, Y. Liu, I.A. Drummond, Dynamic expression of the osmosensory channel trpv4 in multiple developing organs in zebrafish, Gene Expr. Patterns 7 (4) (2007) 480–484.
[22] M. Bossus, G. Charmantier, C. Lorin-Nebel, Transient receptor potential vanilloid 4 in the European sea bass *Dicentrarchus labrax*: a candidate protein for osmosensing, Comp. Biochem. Physiol. Part A Mol. Integr. Physiol. 160 (1) (2011) 43–51.
[23] S. Hori, N. Sakamoto, O. Saitoh, Cloning and functional characterization of medaka TRPV4, Comp. Biochem. Physiol. Part A Mol. Integr. Physiol. 267 (2022), 111182.
[24] X.M. Shang, A.J. Ma, X.A. Wang, et al., Isolation, characterization and expression analysis of TRPV4 in half-smooth tongue sole Cynoglossus semilaevis, J. Oceanol. Limnol. 38 (1) (2020) 294–305.
[25] H.R. Fu, Z.X. Jiao, Y.J. Li, et al., Transient receptor potential (TRP) channels in the Pacific Oyster (*Crassostrea gigas*): genome-wide identification and expression profiling after heat stress between *C. gigas* and *C. angulata*, Int. J. Mol. Sci. 22 (6) (2021) 3222.
[26] H.J. Lee, S.Y. Lee, Y.K. Kim, Molecular characterization of transient receptor potential vanilloid 4 (TRPV4) gene transcript variant mRNA of chum salmon *Oncorhynchus keta* in response to salinity or temperature changes, Gene 795 (2021), 145779.
[27] G.F. Zhang, X.D. Fang, X.M. Guo, et al., The oyster genome reveals stress adaptation and complexity of shell formation, Nature 490 (7418) (2012) 49–54.
[28] L.L. Wang, X.R. Song, L.S. Song, The oyster immunity, Dev. Comp. Immunol. 80 (2018) 99–118.
[29] W.L. Wang, T. Zhang, L.L. Wang, et al., A new non-phagocytic TLR6 with broad recognition ligands from Pacific oyster Crassostrea gigas, Dev. Comp. Immunol. 65 (2016) 182–190.
[30] Z.H. Jia, T. Zhang, S. Jiang, et al., An integrin from oyster *Crassostrea gigas* mediates the phagocytosis toward *Vibrio splendidus* through LPS binding activity, Dev. Comp. Immunol. 53 (1) (2015) 253–264.
[31] E.M. Wagner, Monitoring gene expression: quantitative real-time rt-PCR, Lipoproteins and Cardiovascular Disease (2013) 19–45.
[32] X.R. Song, X.T. Wang, L. Li, et al., Identification two novel nacrein-like proteins involved in the shell formation of the Pacific oyster Crassostrea gigas, Mol. Biol. Rep. 41 (7) (2014) 4273–4278.
[33] Y. Song, X.R. Song, D. Zhang, et al., An HECT domain ubiquitin ligase *Cg*WWP1 regulates granulocytes proliferation in oyster Crassostrea gigas, Dev. Comp. Immunol. 123 (2021), 104148.
[34] B. Yang, Y.K. Jia, Z.H. Jia, et al., The cyclin-dependent kinase 2 (CDK2) mediates hematopoiesis through G1-to–S transition in Chinese mitten crab *Eriocheir sinensis*, Dev. Comp. Immunol. 81 (2018) 156–166.
[35] W.J. Ge, S. Huang, S.J. Liu, et al., A novel Adiponectin receptor (AdipoR) involved in regulating cytokines production and apoptosis of haemocytes in oyster Crassostrea gigas, Dev. Comp. Immunol. 110 (2020), 103727.
[36] M. Pertusa, R. Madrid, Modulation of TRP channels by N-glycosylation and phosphorylation. TRP Channels in Sensory Transduction, Springer, 2015, pp. 73–96.
[37] X. Yao, TRPC, cGMP-dependent protein kinases and cytosolic Ca^{2+} [J]. Transient Receptor Potential Channels, 2007, pp. 527–540.
[38] J.H. Hu, Y.K. Bae, K.M. Knobel, et al., Casein kinase II and calcineurin modulate TRPP function and ciliary localization, Mol. Biol. Cell 17 (5) (2006) 2200–2211.
[39] T.A. White, A.L. Xue, E.N. Chini, et al., Role of transient receptor potential C3 in TNF-α–enhanced calcium influx in human airway myocytes, Am. J. Respir. Cell Mol. Biol. 35 (2) (2006) 243–251.
[40] A. Tirapé, C. Bacque, R. Brizard, et al., Expression of immune-related genes in the oyster *Crassostrea gigas* during ontogenesis, Dev. Comp. Immunol. 31 (9) (2007) 859–873.
[41] G. Haszprunar, A. Wanninger, Molluscs, Curr. Biol. 22 (13) (2012) 510–514.
[42] M. Jemaà, N. Morin, P. Cavelier, et al., Adult somatic progenitor cells and hematopoiesis in oysters, J. Exp. Biol. 217 (17) (2014) 3067–3077.
[43] B.M. Kim, K. Kim, I.Y. Choi, et al., Transcriptome response of the Pacific oyster, Crassostrea gigas susceptible to thermal stress: a comparison with the response of tolerant oyster, Mol. Cell. Toxicol. 13 (1) (2017) 105–113.
[44] M.Q. Li, C.S. Zhang, Y. Zong, et al., Transient receptor potential V channels are essential for glucose sensing by aldolase and AMPK, Cell Metab. 30 (3) (2019) 508–524, e12.
[45] R.A. Pumroy, E.C. Fluck III, T. Ahmed, et al., Structural insights into the gating mechanisms of TRPV channels, Cell Calcium 87 (2020), 102168.
[46] R.G. Scheraga, S. Abraham, L.M. Grove, et al., TRPV4 protects the lung from bacterial pneumonia via MAPK molecular pathway switching, J. Immunol. 204 (5) (2020) 1310–1321.
[47] W. Li, Y. Xu, Z.H. Liu, et al., TRPV4 inhibitor HC067047 produces antidepressant-like effect in LPS-induced depression mouse model, Neuropharmacology 201 (2021), 108834.